OPEN

Neural response during temporal – and spatial luminance contrast processing and its manifestation in the blood-oxygen-level-dependent-signal in striate and extra-striate cortex

Valentine L. Marcar[a,b] and Lutz Jäncke[a]

The primate visual system has been the prime site for investigating the relationship between stimulus property, neural response and blood-oxygen-level-dependent (BOLD)-signal; yet this relationship remains ill-understood. Electrophysiological studies have shown that the ability to visualise a neural response is determined by stimulus property and presentation paradigm. The neural response in the human visual cortex consists of a phasic response processing temporal and tonic response processing spatial luminance contrast. We investigated their influence on the BOLD signal from the visual cortex. To do so, we compared BOLD signal amplitude from BA17 and BA18 of 15 human volunteers to visual patterns varying the size of the active neural population and the discharge activity of this population. The BOLD signal amplitude in both areas reflected the discharge activity of the active neural population but not the size of the active neural population. For identical stimuli, BOLD signal amplitude in BA17 exceeded than that of BA18. This indicates that the BOLD signal reflects the tonic neural neuronal response during spatial luminance contrast processing. The difference in BOLD signal amplitude between BA17 and BA18 is accounted for by differences in neurophysiological and cytoarchitectonic differences between the two areas. Our findings offer an understanding of the relationship between stimulus property, neural response and the BOLD signal by considering the cytoarchitectonic, and neurophysiological make-up between different cortical areas and the influence of a phasic and tonic neural response on local deoxyhaemoglobin concentration. Conversely, differences in BOLD signal between brain structures and stimuli provide cues to the influence of different neurophysiological mechanisms on the neural response. *NeuroReport* 32: 994–1000 Copyright © 2021 The Author(s). Published by Wolters Kluwer Health, Inc.

NeuroReport 2021, **32**:994–1000

Keywords: haemoglobin, luminance, neural response, oxygen extraction fraction

[a]University of Zürich, Chair of Neuropsychology, Institute of Psychology and [b]University Hospital Zürich, Zürich, Switzerland

Correspondence to V.L. Marcar, DPhill, University Hospital Zürich, CCCZ, Rämistrasse 100, 8091 Zürich, Switzerland
Tel: +41442522936; e-mail: valentine.marcar@usz.ch

Received 27 April 2021 **Accepted** 5 May 2021

Introduction

> "Since nothing is so secret or hidden that it cannot be revealed, everything depends on the discovery of those things that manifest the hidden". Paracelsus (1493–1541)

The blood-oxygen-level-dependent (BOLD)-signal-based functional MRI (fMRI) has provided a detailed map of the neural macro network active during perceptual or cognitive processes. Linked to neurovascular coupling, the BOLD signal is a secondary or indirect measure of neural activity with a low temporal resolution [1]. This indirect relationship between BOLD signal and neural activity has proven to be a stumbling block for establishing a quantitative relationship between task difficulty or stimulus property, neural response and the BOLD signal [2,3]. Understanding this relationship is important if inferences about changes in brain activity due to maturation, ageing and disease are to be drawn from differences in BOLD signal [4]. With its anatomical and functional organisation well documented, the visual cortex serves as a favourite site for investigating the relationship between stimulus property, neural response and the BOLD signal. Akin to the visual evoked potential (VEP), the BOLD signal is related to the mass action neural response giving rise to the local field potential, resulting from the sum of excitatory and inhibitory postsynaptic potential acting at the apical dendrites of pyramidal cells [5]. Psychophysical studies [6] point to the presence of a phasic and tonic neural response in the primate visual system and has been drawn on to explain the behaviour of the BOLD signal [7]. Marcar and Jäncke [8] accounted for the appearance of the VEP using a phasic and tonic neural response but concluded that a pattern reversing display impedes the manifestation of the latter in the VEP because a constant neural response results in a direct current shift at the scalp. Given the sluggish nature of the neurovascular response, we wondered whether the BOLD signal is sensitive to the phasic neural response. We set out to ascertain the contribution of the phasic and tonic neural response to the BOLD signal. To do so, we compared BOLD signal

0959-4965 Copyright © 2021 The Author(s). Published by Wolters Kluwer Health, Inc. DOI: 10.1097/WNR.0000000000001677

amplitude in striate and extra-striate cortex to stimuli that varied the size of the active neural population and its discharge activity varying in a graded manner. The former should see a reduction in BOLD signal amplitude as the size of the active neural population increased, the latter an increase in BOLD signal amplitude as the mean discharge activity of the neural population increased.

Materials and methods

Participants

Fifteen healthy adults (nine males) participated in the study. Their mean age was 31 years in the range 19–46 years. All had normal vision and had provided their informed, written consent. Participants were renumerated for participating in the study. All procedures were approved by the local ethics committee (E-08/2006, SPUK – Psychiatry, Zürich, Switzerland).

Apparatus

All measurements took place at the MR centre of the University Hospital Zürich. Functional imaging was performed using a 3T Philips Gyro scanner and a head coil fitted with a small mirror inclined so that the participant, placed in a supine position on the MR-table, was able to see a screen placed at the feet-end of the patient. With the head-coil positioned over their head, participants adjusted their position on the MR-table so that they had a maximum view of the screen. Participants were instructed to move their heads as little as possible and to fixate the middle of a dartboard pattern. These were projected onto the screen through a window using a projector (BASF Plus U2-110) located in the control room. The spatial resolution of the images was 1024 × 768 pixels; the projector refresh rate was 85 Hz, luminance 800 lm and contrast 500:1.

Stimuli

We generated three series of dartboard images. Each dartboard was composed of 9 annuli divided into 16 segments. Neighbouring elements were of opposite luminance contrast. Element size increased between annuli to compensate for the increase in receptive field size with eccentricity [9,10]. The series of dartboard stimuli used are shown in Fig. 1.

In the first series, the size of the dartboard elements varied so that the relative area occupied by the white pixels represented 50, 37.5 and 25% of the area within their circumference. We set the Michelson contrast between light and dark elements between the three series to 99, 66 and 33%. An image with a complementary pattern was generated by rotating the original image by Π radians. During pattern reversing stimulation, the two dartboard images of a complementary pair were presented for 500 ms. At the viewing distance of 3.5 m, each dartboard image subtended a visual angle of 10°. The presentation order of the different patterns was randomised between participants using the Latin square procedure.

Procedure

Blood-oxygen-level-dependent-based functional MR measurements

Prior to each functional imaging measurement, a localiser sequence followed by a high-resolution T1-weighted sequence of seven slices oriented in the sagittal plane was performed. Functional image was performed using a T2*-weighted gradient echo-planar imaging (EPI) sequence with the following parameters: TR = 2000 ms, TE = 35ms, flip angle = 78°, field of view = 220 mm × 220 mm, voxel size = 2.75 × 2.75 × 4.0 mm, inter slice gap = 0 mm. Twenty-six axial slices were oriented parallel to the axis along the anterior and posterior commissure lines. To reduce T1 effects in the BOLD signal, the first three scans of an EPI sequence were discarded. A separate EPI measurement was performed for each of the nine pattern reversing stimuli. During each functional imaging sequence, 20 s of pattern reversing stimulation was followed by 40 s of rest. During the rest period, the same dartboard image remained on the screen. This cycle was repeated five times. At the end of the functional sequence, a high-resolution 3D spin-echo T1-weighted sequence was performed. All images were converted from the native format of the scanner to the statistical parametric mapping (SPM) ANALYZE format.

Functional analysis

Analysis of the functional imaging sequence was performed using SPM8 (Welcome Trust Centre for Neuroimaging, UCL, UK). All functional sequences were preprocessed. This involved motion correction by realigning all images to the first image of a sequence. This was followed by spatially normalising the brain volume of each participant to the montreal neurological index template. This enabled separation of the BOLD signal from BA17 and BA18. Finally, the normalised brain volumes were spatially smoothed using a 5 mm Gauss–Kernel and temporally smoothed using a high-pass filter of 128 Hz.

To identify voxels located in activated brain areas, a first-level analysis was performed on the functional images of a condition using a one-sample Students' *t*-test. Voxels falling within BA17 were identified using the region-of-interest (ROI) tool in the WFUPickatlas [11] and the BA17 mask of the MarsBaR toolbox (Brett *et al.*, 2002) as implemented in SPM. For each time point, the mean signal over all voxels within the boundaries of this ROI was then extracted and stored in the ASCII format. The resulting series represented the BOLD signal during the course of functional measurement of a specific pattern. The BOLD signal for the extra-striate cortex was calculated in an identical manner but using the ROIs for BA18. This was repeated for all nine conditions. When identifying active brain regions, it is customary to perform a post hoc correction. The purpose of such a correction is to reduce the risk of a type I error by correcting the *P* value for multiple testing of spatially distributed voxels. We omitted such a

Fig. 1

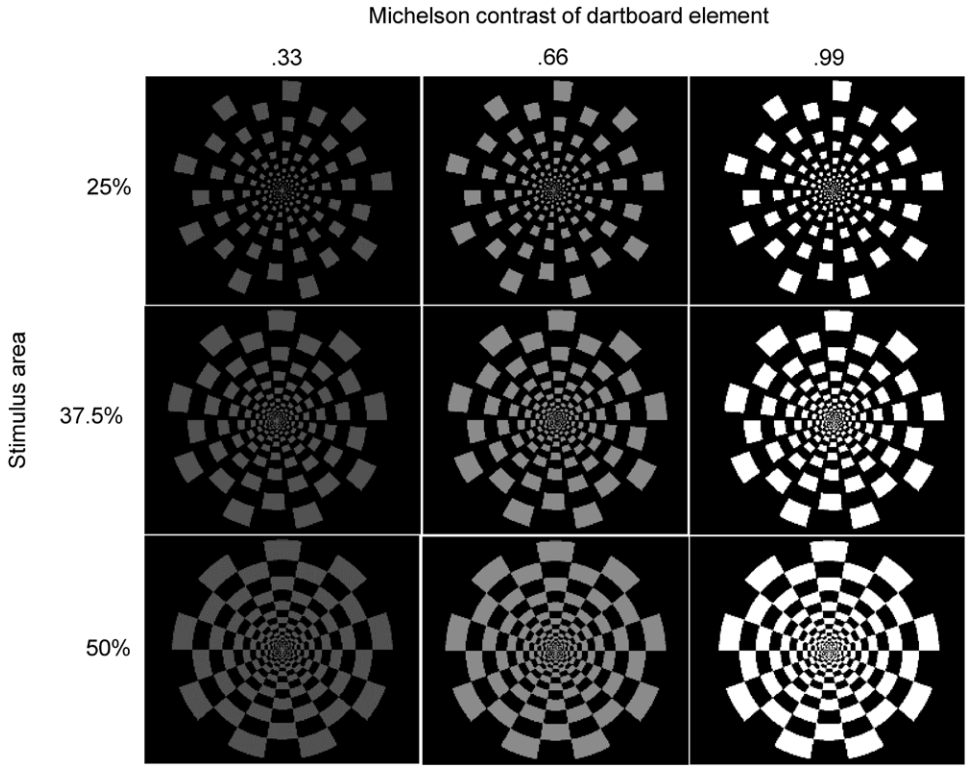

The figure depicts the three dartboard images at the three luminance contrast levels used to generate our pattern reversing stimuli. The relative area undergoing a luminance change increased from the top to the bottom row. The percentage of the relative area undergoing a luminance change is indicated by the number in the DBx identifier. The Michelson contrast of the dartboard elements increases from the left to the right column and is shown above each column.

correction, as in our case, such a correction risked increasing the likelihood of a type I error. Such a correction reduces the set of voxels contributing to the BOLD signal from an ROI to an 'elite' set exhibiting the largest signal change. Such a select set of voxels would yield a stronger activation level within an ROI than the more general activation level obtained when considering all active voxels within an ROI. The glass brain of Fig. 2 shows the active cortical regions obtained following a second-level analysis of the same condition across all participants. To provide an impression of the spatial extent of activation, the data shown were not subjected to a post hoc correction.

Statistical analysis

The mean BOLD signal amplitude of each dartboard stimulus from each participant was compared by a multifactorial analysis of variance (MANOVA) as implemented in the general linear model (GLM) module for repeated measures of SPSS *22* (IBM, Armonk, USA). The factors were: CORTEX (BA17 and BA18), AREA (25, 37.5 and 50) and CONTRAST (33, 66 and 99). To reduce the risk of a type I error, we followed the recommendation of Jafari and Ansari-Pour [12] and accepted $P \leq 0.01$ as indicating a significant difference.

Results

Figure 2 shows the activated brain regions to our stimuli projected onto the glass brain of SPM8. The main focus of activation to each stimulus is located in the occipital lobe.

Figure 3 shows the mean BOLD signal to each stimulus from areas BA17 and BA18.

Table 1 shows the results from the ANOVA of BOLD signal. For the identical dartboard stimulus, BOLD signal amplitude from BA17 was significantly larger than that from BA18. No difference in BOLD signal amplitude was observed for the relative white dartboard area. The luminance contrast of the dartboard elements had a significant influence on BOLD signal amplitude. Two-way interaction CORTEX×CONTRAST was highly significant. All other interactions were NS. A significant liner trend in the within-subject-contrast for AREA and CONTRAST was obtained.

The BOLD signal amplitude from BA17 was significant for CONTRAST but not for AREA. The within-subject contrast revealed a significant linear trend for the factor CONTRAST.

Fig. 2

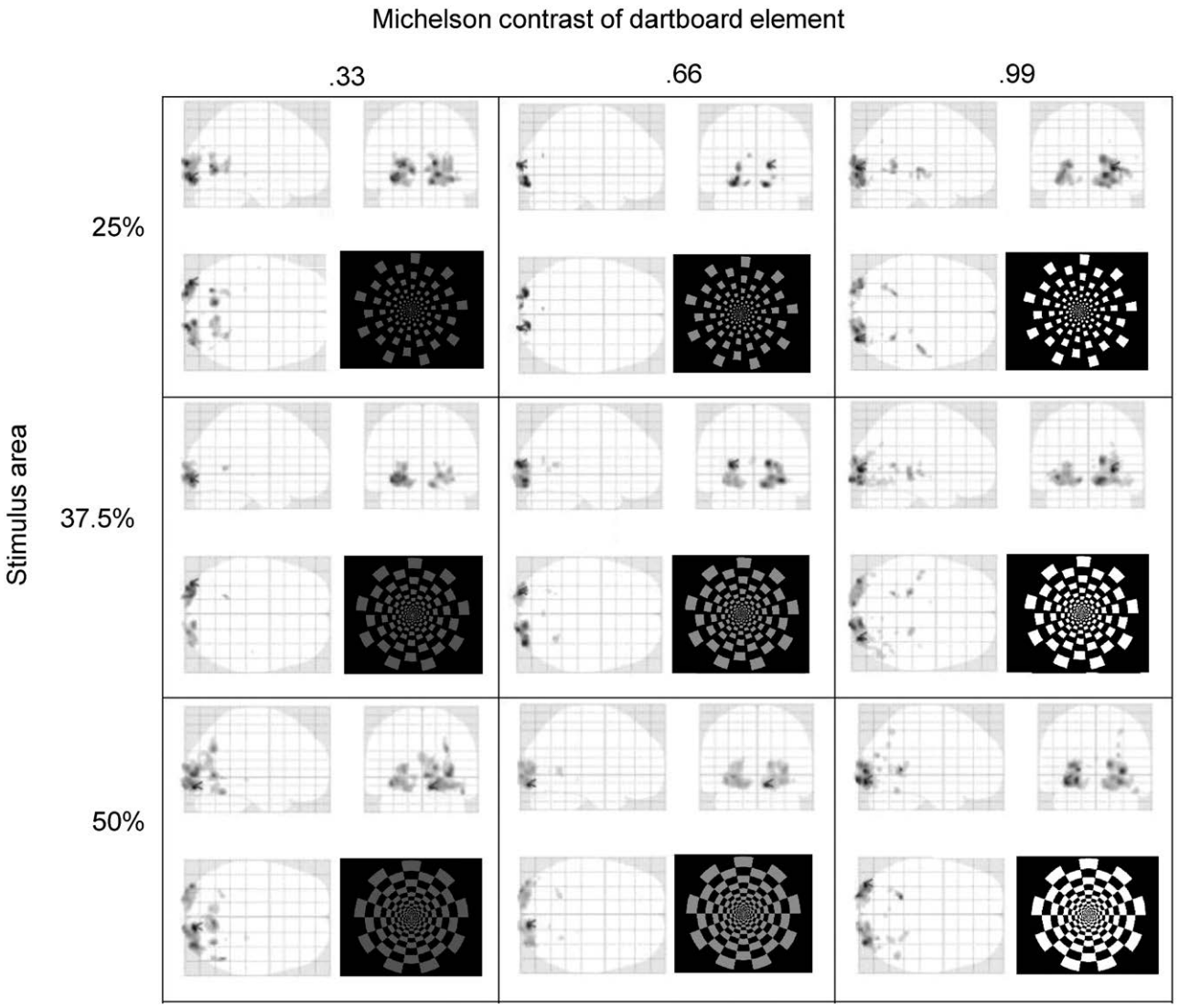

The nine panels of the figure depict the activated brain regions as determined by second-level analysis using SPM8, projected onto a sagittal, axial and coronal view of a glass brain. The red chevron indicates the site of highest blood-oxygen-level-dependent signal. Each of these projections is augmented with the appropriate dartboard images used to generate the pattern reversing stimulus.

The BOLD signal amplitude from BA18 was significant for CONTRAST but not for AREA. The within-subject contrast revealed a significant linear trend for the factor CONTRAST.

Discussion

This discussion is divided into four sections. The first section summarises the main findings. The second briefly outlines the anatomical and functional characteristics of primary (BA17) and secondary (BA18) visual areas. The third discusses the relationship between neural response in the visual system and the BOLD signal. The fourth relates the influence of neural population size and neural discharge activity on the BOLD signal obtained to our stimuli. The focus of this section will be the relationship between BOLD signal amplitude and phasic and tonic neural response during temporal and spatial luminance contrast processing. The fourth and final section deals with the implications of our conclusions on research visualising brain activity using the BOLD signal.

Summary of the findings

The size of the stimulus area undergoing a change in luminance had no influence on BOLD signal amplitude but BOLD signal amplitude in BA17 and BA18 increased as luminance contrast of the elements in our dartboards

Fig. 3

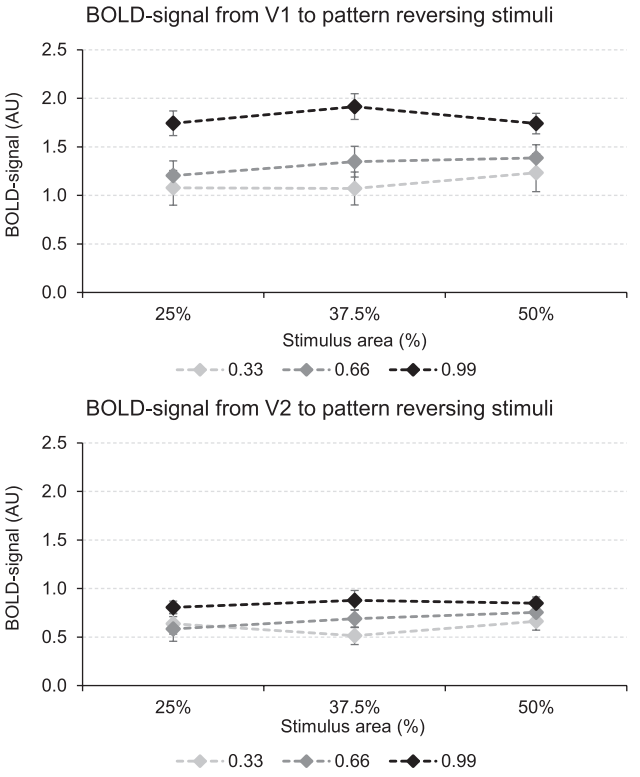

The top panel of the figure depicts the mean blood-oxygen-level-dependent (BOLD) Signal amplitude to the nine stimuli obtained from area BA17. The bottom panel of the figure depicts the mean BOLD signal amplitude to the nine stimuli obtained from area BA18. The error bars indicate the SEM.

increased. BOLD signal amplitude from BA17 was almost double that from BA18.

Characteristics of BA17 and BA18 relevant to our study

This section provides a brief overview of BA17 and BA18 properties most relevant to our study. BA17 and BA18 have similar surface areas [13] and the retinotopic representation of BA18 is the mirror image of BA17. BA17 has a higher neural – [14,15] and vascular density [16] than BA18. BA17 receives up to 40 times more parvocellular than magnocellular input [17] and conveys its output exclusively to BA18. Neurons selective to orientation, motion or chromatic content are located in regions exhibiting distinct affinity for cytochrome oxidase staining in both areas. In BA17, neurons selective to chromatic content are located in cytochrome oxidase-rich 'blobs' and neurons selective to orientation to its cytochrome poor are in inter-blob regions. Neurons selective for motion are found in its granular layers IVa and IVb [18]. In BA18, chromatically selective neurons are found in its thick, cytochrome oxidase-rich stripes (K-stripes), neurons selective to the direction of motion

Table 1 The table contains the result from the GLM analysis of the amplitude of the blood-oxygen-level-dependent-signal from striate and extra-striate cortex to the three dartboard stimuli presented at different luminance contrast

Within-subject-effect	F	Hypothesis df	Error df	*P* value	η^2	Power
CORTEX	52.773	1	14	10^{-3}	0.790	1.000
AREA	2.345	2	13	0.135	0.265	0.390
CONTRAST	24.061	2	13	10^{-3}	0.787	1.000
CORTEX × AREA	0.998	2	13	0.395	0.133	0.187
CORTEX × CONTRAST	17.320	2	13	10^{-3}	0.727	0.998
AREA × CONTRAST	1.293	4	11	0.331	0.320	0.280
CORTEX × AREA × CONTRAST	2.044	4	11	0.157	0.426	0.430
BA17:						
AREA	1.785	2	13	0.207	0.215	0.306
CONTRAST	27.439	2	13	10^{-3}	0.808	1.000
AREA × CONTRAST	1.713	4	11	0.217	0.384	0.364
BA18:						
AREA	2.911	2	13	0.090	0.309	0.470
CONTRAST	10.562	2	13	0.002	0.619	0.962
AREA × CONTRAST	1.213	4	11	0.360	0.306	0.264

in its cytochrome oxidase-rich thin stripes (N-stripes) and neurons selective to orientation in its cytochrome poor, inter-stripes (I-stripes) [19].

Neural response and the blood-oxygen-level-dependent-signal

Marcar *et al.*, [20] concluded that the phasic neural response associated with temporal luminance contrast processing saturated when the Michelson contrast between white and black areas exceeded 30% and that when Michelson contrast remains constant, increasing the size of the active neural population decreases BOLD signal amplitude [21]. Elements in our pattern had a Michelson contrast at or above 30%, so that the phasic neural response to stimuli with the same white area would have been the same. A constant phasic neural response implies that local [HHb], and with it the BOLD signal, is determined by the tonic neural response. The lower BOLD signal amplitude from BA18 indicates that during neural activity [HHb] in its voxels is higher than in the voxels within BA17. This indicates that the higher vascular density in BA17 is able to offset the higher $CMRO_2$ due to its higher neural density. Another factor may be the way magno- and parvocellular signals are processed in the two areas. Magnocellular neurons enter BA17 via its granular lamina IVCα from where they project cytochrome-rich K-stripes of BA18. Parvocellular neurons enter BA17 via its granular layer IVCβ from where chromatically selective neurons project to the cytochrome oxidase 'blobs' and orientation-selective neurons project to the inter-blob regions in the supragranular layers of BA17. During periods of increased neural activity, local [HHb] will be higher in BA18 because $CMRO_2$ in BA18 is higher or because the higher vascular density in BA17 reduces [HHb] levels, leading to a larger BOLD signal.

Implications for relating blood-oxygen-level-dependent-signal to neural response

This final section looks at implications arising from our findings when inferring changes in neural response from differences in BOLD signal. Our approach involves considering a change in neural response to arise from a change in mean discharge activity or a change in the number of active neurons or both. It is an approach based on established physical and neurophysiological properties and yields testable hypotheses for future research. The most important implications of our work concern whether the BOLD signal reflects the neural response to a box-car, an event-related or sparse-sampling paradigm. The BOLD signal from an event-related or sparse-sampling paradigm contains both phasic and tonic neural responses. The BOLD signal from a box-car paradigm however requires careful consideration of how the stimulus paradigm influences the relative contribution of the phasic and tonic neural response to the overall neural response and how the change in cerebral blood flow (CBF) and $CMRO_2$ alters local [HHb], and with it the BOLD signal, in the wake of the ensuing neural response.

Implications for other sensory modalities

Our findings suggest that the ability to infer changes in neural response from changes in stimulus property using the BOLD signal requires knowledge of the neurophysiological make-up of the sensory system and its associated cortical areas. Analogous to the visual system, the somatosensory cortex (S1) receives input from fast-adapting and fast-conducting Pacini and Meissner corpuscle – and slow-adapting and slow-conducting Ruffini receptors and Merkel's disc. The proportion of fast- and slow-adapting fibres entering S1 varies across the body, with the latter representing 61% of the input from the upper and 47% from the lower extremities [22] Noxious stimuli are transmitted via fast-conducting A-fibres and slow-conducting C-fibres. The fast-adapting A-fibres elicit the initial sharp, stabbing pain and the slow-adapting C-fibres the persisting dull, burning pain sensation that follows. Fast-conducting A-fibres make-up 30% and slow conducting C-fibres 70% of the nociceptive input to the brain. Axonal conduction velocity of low-frequency sounds are slower than those of high-frequency sound [23] and the integration time of the former is longer than that of the latter [24]. An extensive discussion of how the BOLD signal relates to the neural response in different sensory systems other than the visual system is both beyond the scope of this article and the knowledge of its authors. Nonetheless, findings that BOLD signal amplitude in superior temporal cortex increased with stimulus presentation rate [25] encourage applying the conclusions of our work to other sensory systems.

Conclusions

Our findings indicate that using differences in BOLD signal amplitude to deduce changes in neural response arising from modifications in stimulus property has to involve an appreciation of the influence of different factors. At the fundamental level a change in neural response may arise from a change in size of the active neural population as well as from a change in discharge activity of a neural population. This paradigm employed during functional MRI measurement plays an important role in determining the relative contribution of a phasic and tonic response to the overall neural response and how the overall neural response influences local [HHb]. Knowledge of the cytoarchitectonic make-up of the brain regions contributing to cognitive or stimulus processing is required to gage the influence of the neural response on CBF and $CMRO_2$ in the area from which the BOLD signal is obtained.

Acknowledgements

The authors thank Martin Warth for performing the fMRI measurements and initial SPM analysis of the functional MRI data.

Conflicts of interest

There are no conflicts of interest.

References

1 Ogawa S, Lee TM, Kay AR, Tank DW. Brain magnetic resonance imaging with contrast dependent on blood oxygenation. *Proc Natl Acad Sci U S A* 1990; **87**:9868–9872.
2 Hillman EM. Coupling mechanism and significance of the BOLD signal: a status report. *Annu Rev Neurosci* 2014; **37**:161–181.
3 Mathias EJ, Kenny A, Plank MJ, David T. Integrated models of neurovascular coupling and BOLD signals: responses for varying neural activations. *Neuroimage* 2018; **174**:69–86.
4 Marcar VL. Is adaptive neuronal plasticity an epiphenomenon of the BOLD-signal? *Restor Neurol Neurosci* 2009; **27**:567–578.
5 Logothetis NK, Pauls J, Augath M, Trinath T, Oeltermann A. Neurophysiological investigation of the basis of the fMRI signal. *Nature* 2001; **412**:150–157.
6 Tolhurst DJ. Sustained and transient channels in human vision. *Vision Res* 1975; **15**:1151–1155.
7 Stigliani A, Jeska B, Grill-Spector K. Differential sustained and transient temporal processing across visual streams. *Plos Comput Biol* 2019; **15**:e1007011.
8 Marcar VL, Jäncke L. To see or not to see; the ability of the magno- and parvocellular response to manifest itself in the VEP determines its appearance to a pattern reversing and pattern oset stimulus. *Brain Behav* 2016; **6**:e00552.
9 Röver J, Bach M. Visual evoked potentials to various check patterns. *Doc Ophthalmol* 1985; **59**:143–147.
10 Zemon V, Ratliff F. Visual evoked potentials: evidence for lateral interactions. *Proc Natl Acad Sci U S A* 1982; **79**:5723–5726.
11 Maldjian JA, Laurienti PJ, Kraft RA, Burdette JH. An automated method for neuroanatomic and cytoarchitectonic atlas-based interrogation of fMRI data sets. *Neuroimage* 2003; **19**:1233–1239.
12 Jafari M, Ansari-Pour N. Why, When and How to Adjust Your P Values? *Cell J* 2019; **20**:604–607.
13 Sincich LC, Adams DL, Horton JC. Complete flatmounting of the macaque cerebral cortex. *Vis Neurosci* 2003; **20**:663–686.
14 Collins CE, Airey DC, Young NA, Leitch DB, Kaas JH. Neuron densities vary across and within cortical areas in primates. *Proc Natl Acad Sci U S A* 2010; **107**:15927–15932.
15 Collins CE, Turner EC, Sawyer EK, Reed JL, Young NA, Flaherty DK, Kaas JH. Cortical cell and neuron density estimates in one chimpanzee hemisphere. *Proc Natl Acad Sci U S A* 2016; **113**:740–745.
16 Weber B, Keller AL, Reichold J, Logothetis NK. The microvascular system of the striate and extrastriate visual cortex of the macaque. *Cereb Cortex* 2008; **18**:2318–2330.

17 Azzopardi P, Jones KE, Cowey A. Uneven mapping of magnocellular and parvocellular projections from the lateral geniculate nucleus to the striate cortex in the macaque monkey. *Vision Res* 1999; **39**:2179–2189.
18 Sato H, Katsuyama N, Tamura H, Hata Y, Tsumoto T. Mechanisms underlying direction selectivity of neurons in the primary visual cortex of the macaque. *J Neurophysiol* 1995; **74**:1382–1394.
19 Sincich LC, Horton JC. The circuitry of V1 and V2: integration of color, form, and motion. *Annu Rev Neurosci* 2005; **28**:303–326.
20 Marcar VL, Baselgia S, Lüthi-Eisenegger B, Jäncke L. Shades of grey; Assessing the contribution of the magno- and parvocellular systems to neural processing of the retinal input in the human visual system from the influence of neural population size and its discharge activity on the VEP. *Brain Behav* 2018; **8**:e00860.
21 Marcar VL, Straessle A, Girard F, Loenneker T, Martin E. When more means less: a paradox BOLD response in human visual cortex. *Magn Reson Imaging* 2004; **22**:441–450.
22 Corniani G, Saal HP. Tactile innervation densities across the whole body. *J Neurophysiol* 2020; **124**:1229–1240.
23 Woods DL, Alain C, Covarrubias D, Zaidel O. Frequency-related differences in the speed of human auditory processing. *Hear Res* 1993; **66**:46–52.
24 Alain C, Woods DL, Covarrubias D. Activation of duration-sensitive auditory cortical fields in humans. *Electroencephalogr Clin Neurophysiol* 1997; **104**:531–539.
25 Binder JR, Rao SM, Hammeke TA, Frost JA, Bandettini PA, Hyde JS. Effects of stimulus rate on signal response during functional magnetic resonance imaging of auditory cortex. *Brain Res Cogn Brain Res* 1994; **2**:31–38.